Evaluation of a Bio-Mechanism by Graphed Static Equilibrium Forces

A.Y. Bani Hashim, N.A. Abu Osman, W.A.B. Wan Abas, and L. Abdul Latif

***Abstract*-**The unique structural configuration found in human foot allows easy walking. Similar movement is hard to imitate even for an ape. It is obvious that human ambulation relates to the foot structure itself. Suppose the bones are represented as vertices and the joints as edges. This leads to the development of a special graph that represents human foot. On a footprint there are point-of-contacts which have contact with the ground. It involves specific vertices. Theoretically, for an ideal ambulation, these points provide reactions onto the ground or the static equilibrium forces. They are arranged in sequence in form of a path. The ambulating footprint follows this path. Having the human foot graph and the path crossbred, it results in a representation that describes the profile of an ideal ambulation. This profile cites the locations where the point-of-contact experience normal reaction forces. It highlights the significant of these points.

Keywords— Ambulation, edge, foot, graph, vertex.

I. Introduction

The unique structural configuration found in human foot allows easy walking (see Fig. 1). Even an ape finds it hard to imitate similar movement. In fact, human foot has a lower total force in joints and muscles than do the ape feet [1]. Figure 2 is a radiograph that shows side view of a typical human foot. By inspection it has 27 bones. The calcaneus bone forms the heel which experiences contact with the ground where the normal reaction force (NRF) is at its peak upon the first step to ambulate.

It is obvious that human ambulation relates to the foot structure itself. Suppose the bones are represented as vertices and the joints as edges so that a special graph is created to represent human foot shown in Fig. 3. Figure 3 and Fig. 4 are both human foot graph but they put labels for vertex and edge respectively. The calcaneus bone is the v_3 vertex. Vertex v_1 is the talus bone, and the edge that joints talus and calcaneus is e_{13}. Notice that there are five trails that branch-off.

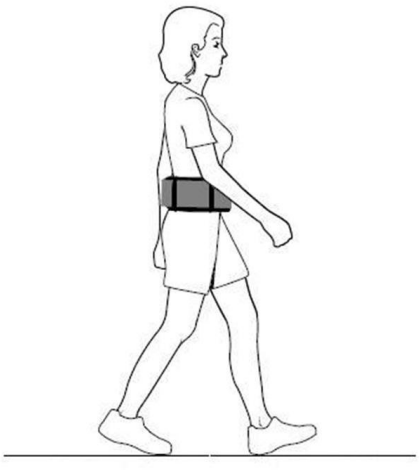

Fig. 1. The above illustration depicts a typical human ambulation. The left foot's heel touches the ground and the reaction force accumulates. This touchdown is the beginning of the sequence in which certain bones actually have contact with the ground. This sequence creates the ambulation path on bones.

Fig. 2. The above picture is a sample human foot radiograph. The side view of this image partially shows the structural arrangement of the 27 bones. It is noted that the structure is somewhat like a leaf spring configuration and a large number of joints seem to act as shock absorbers. Similarly, the curved contact surface that is between the heel and the rest of the bones obviously maintains equilibrium while standing.

A walk from the origin can be made by connecting related vertices. If a walk is to begin from the origin vertex v_1, there are at most five unique walks. Equations (1) to (5) define the walks [2]. Walk-1 begins from the talus and ends at the first digit of the foot. Similarly, walk-5 begins from the talus and end at the fifth digit of the foot.

A.Y. Bani Hashim is with Department of Robotics & Automation, Faculty of Manufacturing Engineering, Universiti Teknikal Malaysia Melaka, Durian Tunggal, 76109 Melaka, MALAYSIA (Phone: 606-3316498; fax: 606-3316431, email: yusairi@utem.edu.my).
N.A. Abu Osman & W.A.B. W.A. are with the Department of Biomedical Engineering, Faculty of Engineering, University of Malaya, 50603 Kuala Lumpur, MALAYSIA (email: azuan@um.edu.my, drirwan1@gmail.com).
L. Abdul Latif is with the Department of Rehabilitation Medicine, Faculty of Medicine, University of Malaya, 50603 Kuala Lumpur, MALAYSIA (email: lydialatif@um.edu.my).

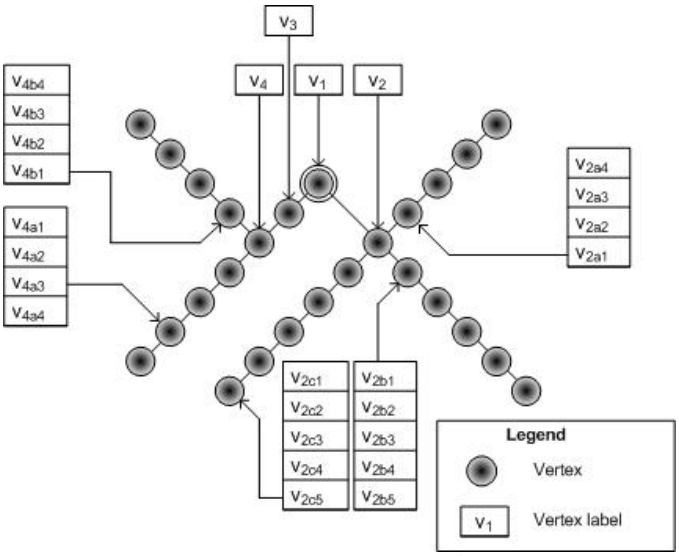

Fig. 3. The above illustration shows the human foot graph that labels vertices where a vertex signifies a bone.

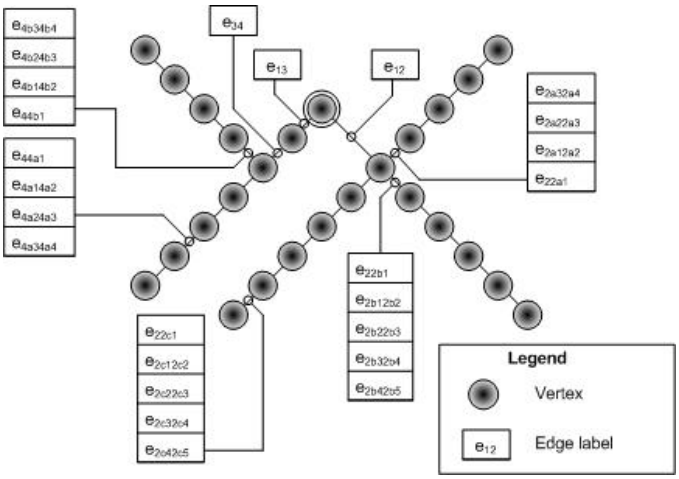

Fig. 4. The above illustration shows the graph that labels edges. An edge connotes a joint.

$$S_{W1} = \left\langle v_1, e_{12}, v_2, e_{22a1}, v_{2a1}, e_{2a12a2}, v_{2a2}, e_{2a22a3}, v_{2a3}, e_{2a32a4}, v_{2a4} \right\rangle \quad (1)$$

$$S_{W2} = \left\langle v_1, e_{12}, v_2, e_{22b1}, v_{2b1}, e_{2b12b2}, v_{2b2}, e_{2b22b3}, v_{2b3}, e_{2b32b4}, v_{2b4}, e_{2b42b5}, v_{2b5} \right\rangle \quad (2)$$

$$S_{W3} = \left\langle v_1, e_{12}, v_2, e_{22c1}, v_{2c1}, e_{2c12c2}, v_{2c2}, e_{2c22c3}, v_{2c3}, e_{2c32c4}, v_{2c4}, e_{2c42c5}, v_{2c5} \right\rangle \quad (3)$$

$$S_{W4} = \left\langle v_1, e_{13}, v_3, e_{34}, e_{44a1}, v_{4a1}, e_{4a14a2}, v_{4a2}, e_{4a24a3}, v_{4a3}, e_{4a34a4}, v_{4a4} \right\rangle \quad (4)$$

$$S_{W5} = \left\langle v_1, e_{13}, v_3, e_{34}, e_{44b1}, v_{4b1}, e_{4b14b2}, v_{4b2}, e_{4b24b3}, v_{4b3}, e_{4b34b4}, v_{4b4} \right\rangle \quad (5)$$

II. Proposition

Proposition. Fig. 1 depicts a typical human ambulation. In completing one cycle of ambulation, a foot undergoes a sequence within an exclusive path that involves thirteen points on the footprint shown in Fig. 5 (above). Point-0 is the initial point depicting the descending foot. Point-1 is when the calcaneus experiences the impulse upon touchdown. So that the sequence for ambulation on the footprint starts from point-0 and ends at point-13 as shown in Fig. 5(below). These points are called the point-of-contacts (POCs). The intensity of ground reaction force that every POC experiences can be represented by a number or color. For example, a POC is assigned a 4 or red if the transpiring NRF acting in opposite is at the largest.

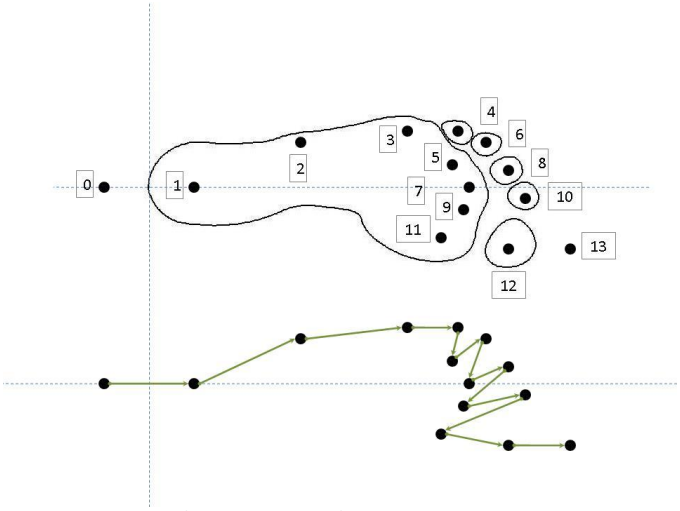

Fig. 5. The point-of-contact on the footprint (above) and the sequence (below).

Equation (6) defines the pattern of ambulating footprint that involves the number of sequences (SEQs), the POCs, and the NRF. Except for sequence-0 and sequence-13, every sequence has at least one POC and a NRF (f_k). At basic standing posture the total weight exerts on the whole foot should equal the total of NRFs.

$$M = \left\{ \left[m_{i,j}, \mathrm{SEQ}_i \times \mathrm{POC}_j \right] \;\middle|\; m_{i,j} = \begin{cases} 4 \equiv \text{Red} & \rightarrow \text{Very Large if } \exists f_k \\ 3 \equiv \text{Violet} & \rightarrow \text{Large if } \exists f_k \\ 2 \equiv \text{Green} & \rightarrow \text{Medium if } \exists f_k \\ 1 \equiv \text{Blue} & \rightarrow \text{Small if } \exists f_k \\ 0 \equiv \text{Gray} & \rightarrow \text{Absent } f_k \end{cases} \right\} \quad (6)$$

Verification. If one cycle of ambulation is to take place the foot should experience NRFs distinctively according to the sequence from point 0 to point 13. So that, during SEQ1 POC1 experiences the largest NRF hence membership function 4, "Very Large", or red. This phenomenon is shown in row two in (8). Deriving one cycle of ambulating foot using (6) results (8) where SEQ0 has zero all cells in row 1 explains that the foot is descending. Upon touching the ground, in row 2, POC1 of SEQ1 has numerical value 4 depicting a "Very Large" NRF is experienced. It follows that the last row having all zeros describing the foot is departing the ground.

$$M_{\text{ambulation}} = \begin{bmatrix} 0&0&0&0&0&0&0&0&0&0&0&0&0&0 \\ 0&4&0&0&0&0&0&0&0&0&0&0&0&0 \\ 0&4&3&3&2&2&2&1&1&1&1&1&1&0 \\ 0&0&4&3&3&2&2&2&1&1&1&1&1&0 \\ 0&0&0&4&3&3&2&2&2&1&1&1&1&0 \\ 0&0&0&0&4&3&3&2&2&2&1&1&1&0 \\ 0&0&0&0&0&4&3&3&2&2&2&1&1&0 \\ 0&0&0&0&0&0&4&3&3&2&2&2&1&0 \\ 0&0&0&0&0&0&0&4&3&3&2&2&2&0 \\ 0&0&0&0&0&0&0&0&4&3&3&2&2&0 \\ 0&0&0&0&0&0&0&0&0&4&3&3&2&0 \\ 0&0&0&0&0&0&0&0&0&0&4&3&3&0 \\ 0&0&0&0&0&0&0&0&0&0&0&4&3&0 \\ 0&0&0&0&0&0&0&0&0&0&0&0&4&0 \\ 0&0&0&0&0&0&0&0&0&0&0&0&0&0 \end{bmatrix} \quad (7)$$

Figure 6 shows the bar plot for the results in 8. It explains the intensity of NRFs of all sequences for an ideal ambulation. In addition, it shows the occurring membership function with respect to the sequence. Both SEQ1 and SEQ12 experience a large NRF onto single POC. For SEQ2, SEQ3, and SEQ4 almost all POCs have contact with the ground.

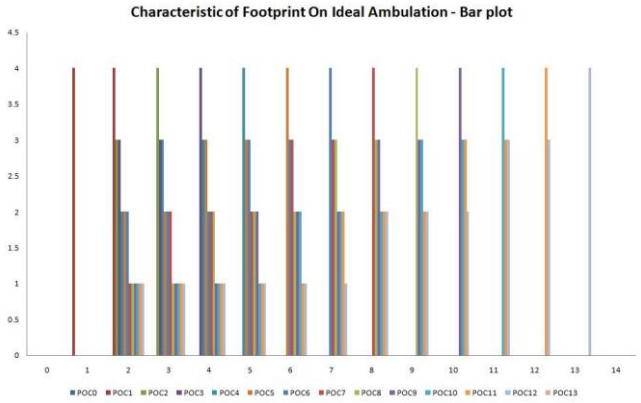

Fig. 6. The bar chart of the sequence of an ideal ambulation

III. Consequence

By observing Fig. 3, Fig. 4, and Fig. 5 it comes by common sense that in (8) to (12) there are POCs that translate into respective NRFs. Equation (8) has F_{11gy} that acts on v_{2a2} nearby e_{2a22a3}. There is higher number of NRFs in (11) and (12). Table 1 lists the bones that relate to vertices and edges with relevant forces. Majority of NRFs are seen to converge around the phalanges. Using (7) and with some mathematical manipulations, the plot in Fig. 7 shows the proposed profile for a normal human ambulation. It is the sum of membership functions with respect to the POC. It shows that POCs 10, 11, and 12 have large concentration of NSFs during one cycle of ambulation.

$$S_{W1}\Big|_{f_k} = \left\langle \begin{array}{l} v_1, e_{12}, v_2, e_{22a1}, v_{2a1}, e_{2a12a2}, \\ v_{2a2}\Big|_{f_{11}}, e_{2a22a3}, v_{2a3}, \\ e_{2a32a4}, v_{2a4}\Big|_{f_{12}} \end{array} \right\rangle \quad (8)$$

$$S_{W2}\Big|_{f_k} = \left\langle \begin{array}{l} v_1, e_{12}, v_2, e_{22b1}, v_{2b1}, e_{2b12b2}, \\ v_{2b2}\Big|_{f_9}, e_{2b22b3}, v_{2b3}, e_{2b32b4}, \\ v_{2b4}, e_{2b42b5}, v_{2b5}\Big|_{f_{10}} \end{array} \right\rangle \quad (9)$$

$$S_{W3}\Big|_{f_k} = \left\langle \begin{array}{l} v_1, e_{12}, v_2, e_{22c1}, v_{2c1}, e_{2c12c2}, \\ v_{2c2}\Big|_{f_7}, e_{2c22c3}, v_{2c3}, e_{2c32c4}, \\ v_{2c4}, e_{2c42c5}, v_{2c5}\Big|_{f_8} \end{array} \right\rangle \quad (10)$$

$$S_{W4}\Big|_{f_k} = \left\langle \begin{array}{l} v_1, e_{13}, v_3\Big|_{f_1}, e_{34}, e_{44a1}, \\ v_{4a1}\Big|_{f_5}, e_{4a14a2}, v_{4a2}, \\ e_{4a24a3}, v_{4a3}, e_{4a34a4}, v_{4a4}\Big|_{f_6} \end{array} \right\rangle \quad (11)$$

$$S_{W5}\Big|_{f_k} = \left\langle \begin{array}{l} v_1, e_{13}, v_3\Big|_{f_1}, e_{34}, e_{44b1}, \\ v_{4b1}\Big|_{f_2}^{f_3}, e_{4b14b2}, v_{4b2}, \\ e_{4b24b3}, v_{4b3}, e_{4b34b4}, v_{4b4}\Big|_{f_4} \end{array} \right\rangle \quad (12)$$

Fig. 8 is the crossbreed graph that fuses the human foot graph of Fig. 3 and the graph of Fig. 5. It shows the path that exists from the start and end points of the ambulating footprint showed in numerical value 0 to 13. It is seen that every stopover point, except 0 and 13, links to a particular vertex and edge. If the foot graph has v_1 decoupled, then there exists two sub graphs. One graph has two branches (G_1) while another has three branches (G_2). Sub graph G_1 contains six POCs so is G_2. Considering six NRFs on G_1, it is fair to infer that G_1 holds the foremost burden as compared to G_2.

TABLE I
LIST OF BONES AND JOINTS THAT EXPERIENCE NORMAL REACTION FORCES

№	Associated bone	Vertex	Nearby edge	f_k
1	Calcaneus	v_3	-	f_1
2	Cuboid-metatarsal	v_{4b1}	e_{44b1}	f_2
3	1st metatarsal-phalanx	v_{4b1}	e_{4b14b2}	f_3
4	2nd metatarsal-phalanx	v_{4a1}	e_{4a14a2}	f_5
5	3rd metatarsal-phalanx	v_{2c2}	e_{2c22c3}	f_7
6	4th metatarsal-phalanx	v_{2b2}	e_{2b22b3}	f_9
7	5th metatarsal-phalanx	v_{2a2}	e_{2a22a3}	f_{11}
8	1st phalanx-phalanx	v_{4b4}	-	f_4
9	2nd phalanx-phalanx	v_{4a4}	-	f_6
10	3rd phalanx-phalanx	v_{2c5}	-	f_8
11	4th phalanx-phalanx	v_{2b5}	-	f_{10}
12	5th phalanx-phalanx	v_{2a4}	-	f_{12}

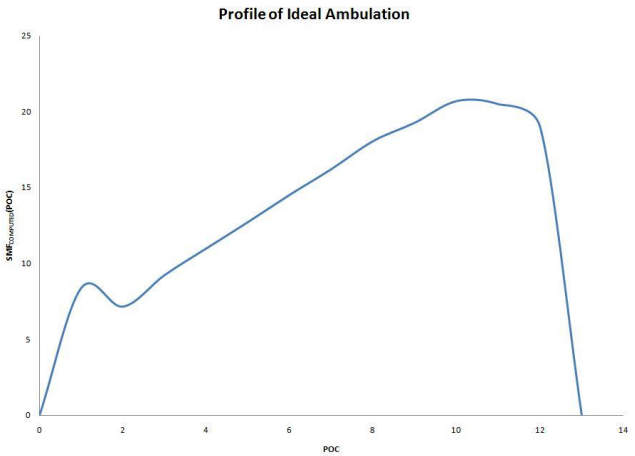

Fig. 7. The plot above is the proposed profile of an ideal ambulation that explains one cycle of ambulating footprint in terms of NRFs that acts on respective POCs.

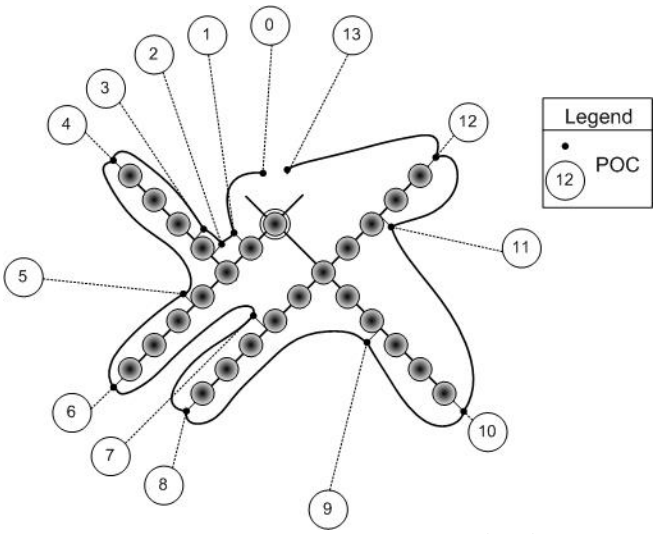

Fig. 8. The illustration above depicts the combination of the foot graph and the sequence of ambulation path on bones. This path initiates from point 0 and end at point 13. Every point has a connection to a vertex.

IV. CONCLUSION

The graph for foot and the sequence of the ambulating footprint have been successfully integrated. This integration has allowed the profile for an ideal human ambulation to be developed. In Fig. 7, the POC2 is the mark in the midsection of the complete ambulation profile. Accordingly, Fig. 3 and Fig. 5 are somewhat related to one another. This is true because in (8) to (12), there is the force component that implicitly cites the location of the NRFs. The ideal ambulation profile as depicted in Fig. 7 explains the significance of the POCs. The area under the curve symbolizes the footprint (see Fig. 5) itself where it has a larger area in the section towards the digits of the foot.

ACKNOWLEDGMENT

This work is funded through the Malaysian Ministry of Higher Education's Fundamental Research Grant Scheme, and is a part of doctoral ongoing research work in the University of Malaya.

REFERENCES

[1] W.J. Wang, R.H. Crompton. "Analysis of the human foot during bipedal standing with implications for the evolution of the foot". *J. of Biomechanics*, vol. 37, pp. 1831-1836, 2004.

[2] A. Y. Bani Hashim, N.A. Abu Osman, W.A.B. Wan Abas. "Formalizing array of foot's bones through a graph". *Second International Conference and Workshops on Basic Science and Applied Sciences & Regional Annual Fundamental Science Seminar 2009 (ICORAFSS 2009)*, Johor Bahru, Malaysia, 2-4 June 2009.

Ahmad Y. Bani Hashim obtained his MS from Universiti Putra Malaysia and BS from Pennsylvania State University both in manufacturing and mechanical engineering. He is senior lecturer in the Department of Robotics & Automation, Faculty of Manufacturing Engineering, Universiti Teknikal Malaysia Melaka (UTeM) since 2003. Prior to joining UTeM he was lecturer in the Department of Automated Systems & Maintenance Technology, Malaysia France Institute. During his tenure at UTeM, he was appointed as visiting scientist at the Intelligent Systems & Robotic Laboratory, Institute of Advanced Technology, Universiti Putra Malaysia for a one-year term. During this period he had developed conceptual idea of a human foot model for use in humanoid robots. Mr. Bani Hashim is now active in evolutionary control systems research and has developed unique control algorithms that imitate the DNA-protein sequence.